Journal of Alloys and Compounds 504S (2010) S515–S518

Contents lists available at ScienceDirect

Journal of Alloys and Compounds

journal homepage: www.elsevier.com/locate/jallcom

Effect of aluminum contents on microstructure and properties of $Al_xCoCrFeNi$ alloys

C. Li, J.C. Li*, M. Zhao, Q. Jiang

Key Laboratory of Automobile Materials (Jilin University), Ministry of Education, and School of Materials Science and Engineering, Jilin University, Changchun 130022, China

ARTICLE INFO

Article history:
Received 3 July 2009
Received in revised form 10 March 2010
Accepted 15 March 2010
Available online 18 March 2010

Keywords:
High entropy alloys
Microstructure
Properties

ABSTRACT

$Al_xCoCrFeNi$ alloys with multiprincipal elements (x values in a molar ratio of 1, 1.5, 2, 2.5 and 3) are prepared by using an arc-melting plus casting method. Their microstructure and mechanical properties are investigated. The results show that the structure of the alloys is an ordered BCC, which is considered as a B2 structure. This result confirms that Al promotes the formation of BCC structure especially when Cu in the alloy is absent. The increase of x leads to distortion of the crystalline lattice and the alloy strengthening. The hardness of the alloys increases with x while the highest hardness (740 HV) is achieved when $x = 3$.

1. Introduction

Usually, alloy systems are based on one principal element as a matrix, such as Fe, Cu, Al, Mg, Ti, etc. This is extended for bulk amorphous alloys where the concept of the multicomponent is taken to drop the melting temperature and to increase the difficulty of crystallization although one essential component of the alloys is still more than 50% [1–7]. It is known that when the principal element has a high solubility; the strength of the solution can increase due to the mechanism of the solution hardening. If the solution structure is kept, the alloy would have a better combination of strength and plastics. As the amount of alloying element increases, intermetallic compounds however are typically formed in the alloys due to the limited solid solubility, which results in enhanced strength at the expense of accompanying embrittlement. To realize the goal of a solution structure, a new alloy design concept, the high entropy (HE) alloy, was explored by Yeh et al. based on the thermodynamic consideration, which consists of a simple FCC or BCC structure [8–10]. The alloys composed of normally n major alloying elements with $n \geq 5$ in equimolar or near-equimolar ratios have better stability due to the contribution of the mixing entropy. Following Boltzmann's hypothesis on the relationship of entropy complexity [8], the configurational entropy change, ΔS_{conf}, during the formation of a solid solution from n elements with equimolar fractions, may be calculated from the following equation:

$$\Delta S_{conf} = -R \ln\left(\frac{1}{n}\right) = R \ln(n) \quad (1)$$

where R is the gas constant. When $n = 5$, $\Delta S_{conf} = 1.61R$, which approaches the magnitude of the melting entropy of the most intermetallic compounds (about $R - 2R$). As results, intermetallic compounds are absent and a single solid solution is built with structures of a single FCC, a single BCC or FCC + BCC [8–15]. Due to the above structural and compositional characteristics, the alloys are ductile and working-hardenable, and have high strength [11]. Thus, the alloys have potential applications as high-temperature structure materials and work tools. Also, due to these possible applications, the properties of the alloys, such as strength, hardness, wear resistance, were investigated [11–15]. To improve the properties of the alloys, the effects of alloying of B, Cr, Ti, Fe, Al and V elements on the structure and properties have been considered [15–19]. Among alloying elements, Al as an interesting element possesses the dualism of metal and nonmetal characteristics duo to its special electronic structure. Al has a nonmetal characteristic when Al is added into metals while Al has a metal characteristic when Al is alloyed into the nonmetal elements. For $Al_xCoCrCuFeNi$ alloy system, an alloy with $x < 0.5$ consists of only an FCC phase [19]. As x increases to 1, AlCoCrCuFeNi alloy are composed of FCC and BCC phases. It was reported that BCC phase of the alloy systems is a spinodal structure that is composed of disordered BCC (A2) and ordered BCC (B2) phases [13]. Although all Cu and Al elements have an FCC structure, the effect of them on the microstructure of HE alloys is however different. The former promotes the formation of FCC structure, while the latter advances the production of

* Corresponding author. Tel.: +86 431 85095371; fax: +86 431 85095876.
E-mail address: ljc@jlu.edu.cn (J.C. Li).

0925-8388/$ – see front matter © 2010 Elsevier B.V. All rights reserved.
doi:10.1016/j.jallcom.2010.03.111

Table 1
The composition of the alloys used in the experiment (at.%).

Alloy no.	Co	Ni	Cr	Fe	Al	Atomic ratio
1	20	20	20	20	20	$Al_1CoCrFeNi$
2	18.2	18.2	18.2	18.2	27.2	$Al_{1.5}CoCrFeNi$
3	16.7	16.7	16.7	16.7	33.2	$Al_2CoCrFeNi$
4	15.4	15.4	15.4	15.4	38.4	$Al_{2.5}CoCrFeNi$
5	14.3	14.3	14.3	14.3	42.8	$Al_3CoCrFeNi$

a BCC structure [13]. Since Cu and Al are present synchronously in AlCoCrCuFeNi alloy systems, their effect cannot be clearly distinguished. It is unknown whether or not a single FCC phase arises even if Al% content is small at absence of Cu. Also, whether the BCC phase is a partly ordered phase, namely a B2 structure, which is unclear although a B2 phase formation could be reasonable due to the existence of Al and Ni and their strong compound formation tendency. Moreover, the influence mechanism of Al on the microstructure and properties of the alloys need to be studied systematically.

In light of the above discussion, in this contribution, $Al_xCoCrFeNi$ alloys with different Al concentrations are fabricated. The corresponding microstructures and mechanical properties are measured to find the effect of Al on the alloy structure under a case without Cu in the alloying systems.

2. Experimental methods

$Al_xCoCrFeNi$ alloys are prepared by a vacuum furnace under argon atmosphere. The rod ingot of the alloy with a diameter of 6 mm is obtained in a cold copper hearth. The corresponding cooling rate is about 10^3 K/s. Table 1 shows the composition of the alloys. The phase structure analysis of the samples was made by Rigaku D/max 2500 X-ray diffractometer at 50 kV and 250 mA. Scanning angles ranged from 20° to 110° with a scanning rate of 5°/min. The microstructure of the alloys was observed by optical micrographs and transmission electron microscope (TEM) respectively. The selected area composition analysis of the samples was carried out by an energy dispersive spectrometry (EDS). The hardness of the samples was determined by a Vickers hardness instrument. Vickers' load was 200 g with a loading time of 15 s. The density was determined by a balance with a precision of 0.01 mg based on Archimedes's principle.

3. Results and discussion

Fig. 1 shows X-ray phase analysis results of the alloys with different *x*. All alloys consist of a single ordered BCC phase with a superlattice peak as shown in early literatures [19]. The intensity of the diffraction peak decreases with increasing of *x* because the addition of Al induces aberrance of the crystalline lattice. Compared

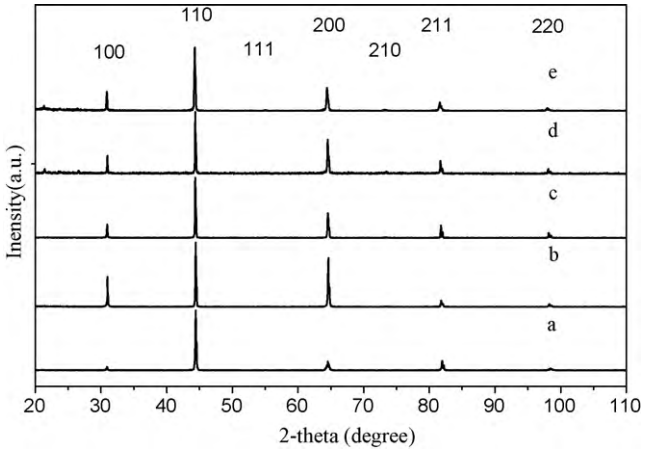

Fig. 1. X-ray diffraction curve analysis of the alloys with different aluminum contents. (a) $Al_1CoCrFeNi$ alloy, (b) $Al_{1.5}CoCrFeNi$ alloy, (c) $Al_2CoCrFeNi$ alloy, (d) $Al_{2.5}CoCrFeNi$ alloy, and (e) $Al_3CoCrFeNi$ alloy. All the X-ray diffraction peaks of HE alloys belong to ordered BCC phase.

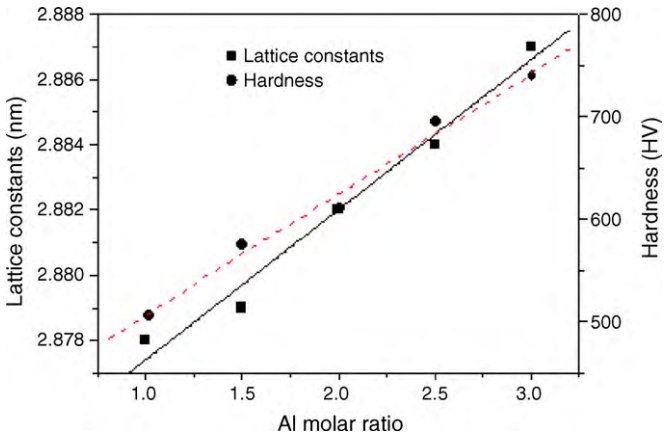

Fig. 2. Lattice constants and Vickers hardness of $Al_xCoCrFeNi$ alloys with different *x*.

with other elements in the alloy, Al element combines with Ni element to form a BCC NiAl ordered solid solution, while the other elements dissolve in the solid solution. The lattice constant of the alloys increases from 2.878 to 2.887 nm with increasing of *x* since the atomic radius of Al is larger than the other elements in the alloys as shown in Fig. 2. The increase of Al content not only introduces the lattice strain, but also affects the structure of the alloys.

Fig. 2 also gives the hardness of the alloys as a function of Al molar ratio. The alloys possess high hardness, which increases from 506 to 740 HV as *x* increases. It is known that the chemical mixing enthalpy of Al–Ni, Al–Co, Al–Fe and Al–Cr are $-30\,kJ\,mol^{-1}$, $-24\,kJ\,mol^{-1}$, $-10\,kJ\,mol^{-1}$ and $-6\,kJ\,mol^{-1}$ respectively. However, the chemical mixing enthalpy of Cr–Ni, Cr–Co, Cr–Fe, Co–Fe, Ni–Fe and Co–Ni are $3\,kJ\,mol^{-1}$, $8\,kJ\,mol^{-1}$, $13\,kJ\,mol^{-1}$, $13\,kJ\,mol^{-1}$, $12\,kJ\,mol^{-1}$ and $17\,kJ\,mol^{-1}$ respectively [20]. This result implies that the combinative force of Al element with other elements in the alloy is the strongest among the combinative force of the elements in the alloys. In addition, atomic size of Al is biggest in the all elements of the alloys, so that the aberrance of crystal lattice increases with increasing *x*. The distortion of crystal lattice and possibly the enhancement of the bond strength of Al with other elements bring out the increase the hardness of the alloy.

Fig. 3 presents the microstructure of the alloys with different *x*, which is a typical dendritic crystal structure. However, the morphologies of dendrite and interdendrite are diverse in this alloy system, which implies a difference in composition in distinct solidification zones due to the growth sequences. As *x* increases, the morphology of the microstructure varies from a cotton-boll shape, cauliflower, spinodal or a petal to a fishbone shape respectively. Also, the grains coarsen with increasing *x*.

TEM diffraction measurement is shown in Fig. 4 where the primary ◯ dots denote B2 structure while the other four □ dots show FCC or L12 one. Since FCC or L12 structure cannot be observed in X-ray diffraction experiment, the percentage of FCC or L12 structure should be smaller than 5%. The existence of or FCC or L12 should be related to the inhomogeneous distribution of Al in the alloy where Al content is small, as reported in references [21,22]. B2 should be a more possible structure since Al and Ni as essential components have a high formation enthalpy H^c_{AlNi}, which leads to that Al and Ni should hold the sites of center and corner in B2, respectively. While the other components substitute Al and Ni depending on their relative differences of the electronegativity value *I* and the atomic radius *r*. Due to the similar *I* and *r* values of Co, Ni and Fe in 1.88, 1.91, 1.83, and in 1.25 Å, 1.25 Å, 1.24 Å, respectively, Fe and Co could take up the site of Ni in a B2 structure. On the other hand, *I* and *r* values of Cr and Al are 1.61, 1.66 and 0.143 nm, 0.125 nm, respectively, and Cr may thus occupy the site of Al. As results, BCC

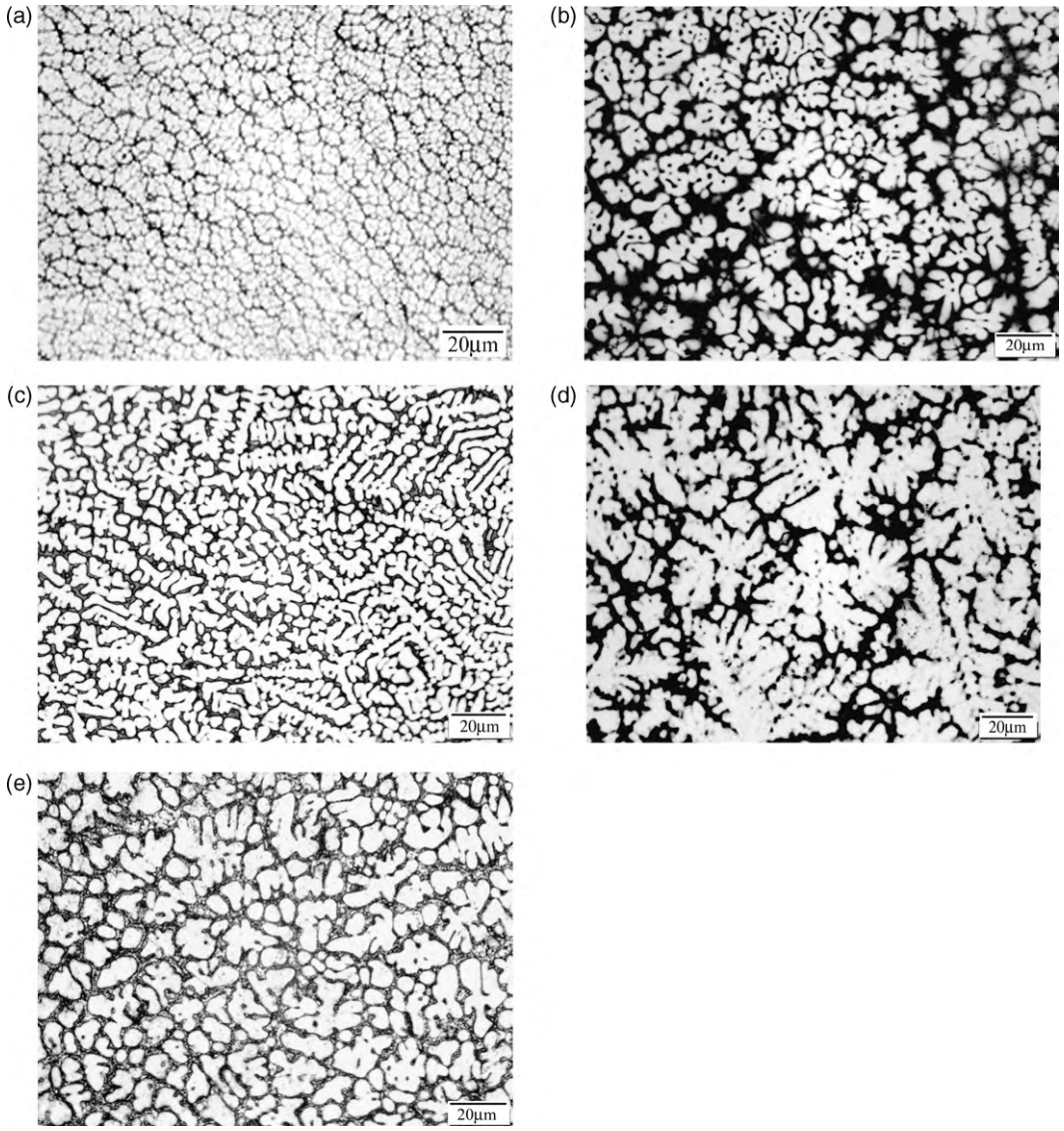

Fig. 3. Optical micrographs of the alloys with different *x*. (a) $Al_1CoCrFeNi$ alloy, (b) $Al_{1.5}CoCrFeNi$ alloy, (c) $Al_2CoCrFeNi$ alloy, (d) $Al_{2.5}CoCrFeNi$ alloy, and (e) $Al_3CoCrFeNi$ alloy.

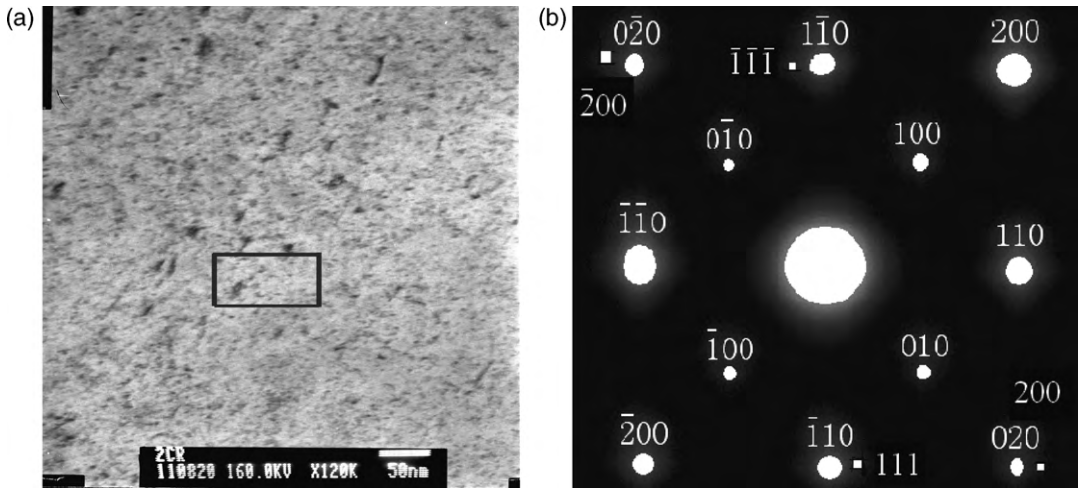

Fig. 4. TEM micrograph and diffraction pattern of $Al_1CoCrFeNi$ alloy. (a) TEM micrograph, (b) Diffraction pattern, the primary ○ dots denote B2 structure while the other four □ dots denote FCC or L12 one, which is absent in the X-ray diffractions.

Table 2
Dendritic (D) and interdendritic (I) compositions determined by EDS (at.%).

Alloy		Co	Ni	Cr	Fe	Al
$Al_1CoCrFeNi$	D	19.56	20.65	20.29	19.87	19.63
	I	20.02	21.07	20.41	20.02	18.48
$Al_{1.5}CoCrFeNi$	D	18.48	19.07	18.12	19.06	25.28
	I	18.16	17.54	20.57	20.97	22.66
$Al_2CoCrFeNi$	D	17.77	19.43	15.60	17.85	29.35
	I	22.88	23.23	20.42	20.93	10.53
$Al_{2.5}CoCrFeNi$	D	18.47	19.07	18.12	19.04	25.2
	I	18.07	15.95	22.26	21.55	22.17
$Al_3CoCrFeNi$	D	15.67	16.13	15.27	15.89	36.86
	I	16.34	17.08	16.45	16.73	33.67

phase should be a B2 phase while other elements are dissolved in the phase [20].

Table 2 is the element distribution in the alloys determined by EDS. The result shows that the element distribution is almost in agreement with the element ratio of the alloys at the location of the dentrite and that of the interdentrite. Under a condition of rapid solidification, four of the five elements in the alloys are expected to be statistically distributed in BCC lattice according to the probability of occupancy except Al since Al could predominate to pair with other four elements as illustrated above.

4. Summary

$Al_xCoCrFeNi$ HE alloys have a single BCC structure due to the absence of element Cu in HE alloys. Since the strongest formation enthalpy between Al and Ni, the BCC structure is dominant by Al and Ni while other elements are dissolved in the phase. BCC phase has an ordered B2 structure. The results confirm that Al promotes the formation of BCC structure especially when Cu is absent in the alloying system. As x increases, the crystal lattice constant of the alloys increases, which brings out a significant increase in hardness. The highest hardness of the alloys reaches about 740 HV.

Acknowledgements

The authors gratefully acknowledge the financial supports from NNSFC (Grant No. 50571040), National Key Basic Research and Development Program (Grant No. 2010CB631001), and Program for Changjiang Scholars and Innovative Research Team in University.

References

[1] A. Takeuchi, A. Inoue, Mater. Trans. JIM 41 (2000) 1372.
[2] A. Inoue, K. Ohtera, K. Kita, T. Masumoto, Jpn. J. Appl. Phys. 27 (1988) L2248.
[3] H.W. Kui, A.L. Greer, D. Turnbull, Appl. Phys. Lett. 45 (1988) 616.
[4] A. Inoue, T. Zhang, T. Masumoto, Mater. Trans. JIM 31 (1991) 177.
[5] A. Peker, W.L. Johnson, Appl. Phys. Lett. 63 (1993) 2342.
[6] R. Akatsuka, T. Zhang, M. Koshiba, A. Inoue, Mater. Trans. JIM 40 (1999) 58.
[7] T. Zhang, A. Inoue, Mater. Trans. JIM 39 (1998) 857.
[8] J.W. Yeh, S.K. Chen, S.J. Lin, J.Y. Gan, T.S. Chin, T.T. Shun, C.H. Tsau, S.Y. Chang, Adv. Eng. Mater. 6 (2004) 299.
[9] B. Cantor, I.T.H. Chang, P. Knight, A.J.B. Vincent, Mater. Sci. Eng. A 375–377 (2004) 213.
[10] P.K. Huang, J.W. Yeh, T.T. Shun, S.K. Chen, Adv. Eng. Mater. 6 (2004) 74.
[11] Y.J. Zhou, Y. Zhang, T.N. Kim, G.L. Chen, Mater. Lett. 62 (2008) 2673.
[12] Y.S. Huang, L. Chen, H.W. Lui, M.H. Cai, J.W. Yeh, Mater. Sci. Eng. A 457 (2007) 77.
[13] S. Varalakshmi, M. Kamaraj, B.S. Murty, J. Alloys Compd. 460 (2008) 253.
[14] C.C. Tung, J.W. Yeh, T.T. Shun, S.K. Chen, Y.S. Huang, H.C. Chen, Mater. Lett. 61 (2007) 1.
[15] C. Li, J.C. Li, M. Zhao, L. Zhang, Q. Jiang, Mater. Sci. Technol. 24 (2008) 376.
[16] Y.J. Zhou, Y. Zhang, J.A. Zhang, G.L. Chen, Appl. Phys. Lett. 90 (2007) 181904.
[17] M. Chen, Y. Liu, Y.X. Li, Acta Metall. Sinica 43 (2007) 1020.
[18] U.S. Hsu, U.D. Hung, J.W. Yeh, S.K. Chen, Y.S. Huang, C.C. Yang, Mater. Sci. Eng. A 469 (2007) 403.
[19] Y.J. Zhou, Y. Zhang, Y.L. Wang, G.L. Chen, Mater. Sci. Eng. A 454 (2007) 260.
[20] F.R. de Boer, R. Boom, W.C.M. Mattens, A.R. Miedema, A.K. Niessen, Cohesion in Metals: Transition Metals Alloys, North-Holland, Amsterdam, 1988.
[21] C. Li, M. Zhao, J.C. Li, Q. Jiang, J. Appl. Phys. 104 (2008) 113504.
[22] Y.P. Wang, B.S. Li, H.Z. Fu, Adv. Eng. Mater. 11 (2009) 641.